TELO2 induced progression of colorectal cancer by binding with RICTOR through mTORC2

ZHENG GUO[1,2*], XIUFANG ZHANG[3*], HUABIN ZHU[3*], NANYING ZHONG[3], XIAONING LUO[1,2],
YU ZHANG[1,2], FUPING TU[1,2], JINGHUA ZHONG[1,2], XIANGCAI WANG[1,2], JUE HE[4,5] and LI HUANG[1,2]

[1]Department of Oncology, and [2]Clinical Cancer Research Center of Jiangxi Province, First Affiliated Hospital of
Gannan Medical University, Gannan Medical University; [3]First School of Clinical Medicine, Gannan Medical University;
[4]Department of Pathology, First Affiliated Hospital of Gannan Medical University, Gannan Medical University;
[5]School of Basic Medicine, Gannan Medical University, Ganzhou, Jiangxi 341000, P.R. China

Abstract. Colorectal cancer (CRC) is a common cancer worldwide, and its treatment strategies are limited. The underlying mechanism of CRC progression remains to be determined. Telomere maintenance 2 (TELO2) is a mTOR-interacting protein. Both the role and molecular mechanism of TELO2 in cancer progression remain unknown. In this study, the gene expression database of normal and tumor tissue, in addition to western blot analysis, and immunohistochemistry (IHC) were used to determine the expression and location of TELO2 in CRC and normal tissues. Clinical features of a tissue array were collected and analyzed. WST-1, soft agar, flow cytometry, wound healing, and invasion assays were employed to verify the role of TELO2 in the growth, cell cycle, migration, and invasion of CRC cells. The correlation between TELO2 and RICTOR (rapamycin-insensitive companion of mTOR) was analyzed by bioinformatics, IHC, and immunoprecipitation. Normal and serum-deprived cells were collected to detect the protein level of TELO2 and its downstream effectors. The results revealed that TELO2 was significantly upregulated in CRC, and TELO2 inhibition significantly restrained the growth, cell cycle, and metastasis of CRC cells. TELO2 overexpression correlated with age, lymph node metastasis, and TNM stage of CRC patients. In addition, TELO2 was positively correlated with RICTOR in CRC and induced tumor progression mainly via RICTOR with serum in culture.

Correspondence to: Dr Zheng Guo, Department of Oncology, First Affiliated Hospital of Gannan Medical University, Gannan Medical University, Ganzhou, Jiangxi 341000, P.R. China
E-mail: jen716@qq.com

*Contributed equally

RICTOR induced the degradation of TELO2 upon serum deprivation in an mTOR-independent manner. These findings indicate that TELO2 promotes tumor progression via RICTOR in a serum-dependent manner, which may be a potential therapeutic target for CRC.

Introduction

Colorectal cancer (CRC) is one of the most common types of cancer worldwide, especially in China within the last decade (1). CRC progression, from adenoma to adenocarcinoma, is a multistep process (2). CRC results from a series of genetic and epigenetic alterations in key growth regulatory genes, which endow the colorectal cells with proliferative, survival, and metastatic advantages (3). The median overall survival (OS) of metastatic CRC (mCRC) is less than 3 years. Chemotherapy, radiotherapy, targeted therapy, and immunotherapy are mainly palliative treatments (4). Therefore, there is a need for more efficacious strategies to prolong the OS of mCRC.

Telomere maintenance 2 (TELO2, also known as tel2) was first identified in Saccharomyces cerevisiae and was required in telomere length regulation and telomere position (5). TELO2 binds with phosphatidylinositol 3-kinase-related kinase (PIKK) family members, including ATM (ataxia telangiectasia mutated), ATR (ATM- and rad3-related), and mammalian target of rapamycin (mTOR) (6), and it maintains the stability of PIKKs, which leads to the translation, growth, and autophagic regulation of cells (7,8). The PI3K/Akt/mTOR pathway is frequently dysregulated in CRC patients, and the therapeutic potential of targeting mTOR in the treatment of CRC is rational and has been shown to improve disease progression (9). With regard to mTOR, TELO2 is not only critical for protein stability, but it is also essential for the integrity of mTOR complexes (10,11). Degradation of TELO2 promotes the survival of multiple myeloma under growth factor withdrawal (12). Although there are several reports indicating that TELO2 demonstrates an oncogenic profile in solid tumors, such as breast cancer (13) and high-grade gliomas (14), the role and molecular mechanism of TELO2 in CRC tumorigenesis have yet to be defined. A study on TELO2 in CRC

demonstrates that a germline mutation of TELO2 regulated the senescence pathway and is related to sessile serrated adenomas and adenocarcinoma progression (15). Additionally, rapamycin-insensitive companion of mTOR (RICTOR), a specific adaptor of mTORC2 (16), plays an important role in cancer cell proliferation, autophagy, migration, and invasion via activation of protein kinase B (Akt) (17,18) and is positively correlated with prognosis in CRC (19). Thus, we hypothesized that TELO2 is important in the development of CRC via mTOR and RICTOR. In this study, we performed bioinformatics combined with *in vitro* experiments and analysis of clinical characteristics of CRC patients in order to characterize the effect of TELO2 on CRC progression.

Materials and methods

Cell lines and tissue specimens. The anti-TELO2 antibody (ab122722, 1:500 dilution) was purchased from Abcam (Cambridge). The anti-RICTOR antibody (cat. no. A300-459A-M, 1:1,000 dilution) was purchased from Bethyl (Montgomery). Antibodies against mTOR (cat. no. 2972, 1:1,000 dilution), RAPTOR (cat. no. 4978, 1:1,000 dilution), phosphorylated-Akt (Ser473, cat. no. 4051, 1:500 dilution), Akt (cat. no. 9272, 1:500 dilution), S6K1pT389 (cat. no. 9204, 1:500 dilution), S6K1 (cat. no. 9202, 1:500 dilution), 4E-BP1pS65 (no. 9451, 1:500 dilution), 4E-BP1 (no. 9452, 1:500 dilution), tubulin (cat. no. 2146, 1:1,000 dilution), ubiquitin (cat. no. 43124, 1:1,000 dilution), and Myc-tag (cat. no. 2276, 1:1,000 dilution) were obtained from Cell Signaling. The anti-β-actin antibody (cat. no. A1978, 1:2,000 dilution) was purchased from Sigma (Milwaukee). LoVo cells, a human colorectal cancer cell line (CBP60032, Cobioer, Shanghai), was selected from the GENT2 database, authenticated by STR analysis (September, 2016) and maintained in RPMI-1640 basic media containing 10% fetal calf serum (FBS, no. 10100, Gibco, Shanghai) at 37°C with 5% CO_2. Serum-deprived conditions were defined as maintaining cells in RPMI-1640 media with 0.02% FBS. Four pairs of CRC tissues (on the edge of cancerous specimens without necrosis) and normal adjacent tissues (2 cm away from the cancer margin) were collected from resected surgical specimens in our hospital from April, 2019 to December, 2019. There were 2 males and 2 females, with an age range of 53 to 81. Tissue array slides (no. HColA180Su10) were purchased from Superchip (Shanghai, China). All of the patients signed informed consent for the use of their tissues, and the Institutional Review Committee of Gannan Medical University (Ganzhou, Jiangxi) approved this study (no. 2018023).

Tissue array and immunohistochemistry (IHC). For IHC experiments, tissue array slides were used with 100 CRC tissue spots and 80 adjacent normal tissue spots. Endogenous peroxidase activity was blocked by incubation with hydrogen peroxide, and antigen retrieval was then performed by incubation in a pepsin solution at 37°C. The sections were then incubated with an anti-TELO2 antibody (1:500) or anti-RICTOR (1:4,000) antibody at 4°C overnight, followed by incubation with the biotin-linked anti-rabbit IgG (Dako) and then with the ABC complex (ab8647; Cambridge). The staining sections were then reviewed and scored as follows

by a pathologist with over 15 years of experience: Cells with <10% staining were scored as negative staining (-, 1); cells with 10-49% staining were scored as (+, 2); cells with 50-74% staining were scored as (++, 3); and cells with 75-100% staining were scored as (+++, 4). The staining color was scored as light-yellow particle (1), brown-yellow particle (2), and brown particle (3). The final score was defined as staining number score multiplied by staining color score (20). The scores of negative expression were between 0 and 5, and the scores that exceeded 5 were identified as positive expression.

RNA isolation and quantitative PCR. Cells were harvested and total RNA was extracted from LoVo cells (transfected with scramble siRNA or RICTOR siRNA) using TRIzol reagent (no. 15596026; Gibco) as previously described (21). qPCR was performed using Power SYBR-Green PCR Master Mix (no. 4309155; Applied Biosystems). The qPCR conditions were 5 min at 95°C, followed by 50 cycles of 95°C for 15 sec, 56°C for 30 sec, and 72°C for 40 sec, 72°C for 5 min was included for a final extension. The primer sequences used in RT-PCR were as follows: TELO2 forward, 5'-GTCCCTGAA GCGGTATCTCG-3' and reverse, 5'-TGCTGGCAAGACATC TGAGG-3' (107 bp); GAPDH forward, 5'-GTCAACGGATTT GGTCGTATTG-3' and reverse, 5'-CTCCTGGAAGATGGT GATGGG-3' (216 bp).

Transient transfection and generation of stably transfected cells. Knockdown of RICTOR expression was performed by transfecting cells with siRNA duplexes (sc-61478; Santa Cruz Biotechnology) using Lipofectamine 3000 (Thermo Fischer Scientific). Scrambled RNA (scr-siRNA) was used as a negative control. The TELO2 shRNA plasmid (sc-93308-SH) was purchased from Santa Cruz Biotechnology. The pLPC-Myc-TELO2 (no. 22802) plasmid was purchased from Addgene. The indicated plasmids were transfected into LoVo cells. Transfects were cultured in RPMI-1640 medium supplemented with puromycin (Medchemexpress LLC) to generate stable cell lines.

Western blot analysis and co-immunoprecipitation (Co-IP). Whole cell lysates and cytoplasmic protein were prepared following the instructions of a protein extraction kit from Sangon Biotech (C006255 and C510001). For western blot analysis, 30 µg of whole protein lysates was used to detect the indicated protein, 4-12% NuPAGE Bis-Tris gel (NP0322BOX, Invitrogen) was used for electrophoresis. STRING database (https://string-db.org) was used for predicting the protein combination before experiments. For Co-IP assay, 1% Triton (strong lysis buffer which can depolymerize the mTOR complex) or CHAPS (mild buffer which can maintain the integrated mTOR complex) lysis buffer was used. After pre-incubation with protein G PLUS-Agarose beads (20423, Thermo Fisher Scientific), an equal amount of protein (500 µg) was incubated with the indicated antibodies (1 µg, RICTOR or TELO2). 1% Triton or CHAPS buffer was used to wash beads at 4°C, 200 x g three times. Then 1% of the input was loaded to detect the protein level. PVDF (LC2002; Thermo Fisher) was used as transmembrane. ImageJ software was used to scan the grey scores of images. Cycloheximide (CHX; Calbiochem) was used for protein chasing experiment.

WST-1 cell proliferation assay. Each group of isolated tumor cells was seeded into 5 wells of a 96-well plate and incubated for 24, 48, or 72 h in RPMI-1640 containing 10% FBS. After washing, fixing, and permeabilizing the cells, 10 μl of WST-1 was added to each well and incubated at 37°C for 4 h. The absorbance at 490 nm was measured with a microplate reader (Thermo Fisher Scientific, Vantaa, Finland). The survival rate was calculated using the proportion between the absorbance of different cells.

Anchorage-independent cell growth assay. LoVo cells (1.25x10³) transfected with different plasmids were seeded into medium with 0.35% agar and plated in triplicate on plates containing a 0.7% agar base. Colonies were stained with Coomassie Blue (no. sc-24972; Santa Cruz Biotechnology). Colonies containing at least 50 cells were counted using Photoshop software (Adobe Systems).

Cell cycle analysis. At 48 h post-transfection, LoVo cells with scramble shRNA or TELO2 shRNA was digested with trypsin (no. 25300054; Thermo Fischer Scientific), washed twice with PBS, and collected by centrifugating at 1,000 x g for 5 min. For cell cycle analysis, the cells were fixed with pre-cooled 70% ethanol at 4°C overnight and digested with 200 mg/ml ribonuclease A (KeyGen BioTech, KGA511) at 37°C for 30 min. The cells were then stained by the addition of 100 μl of propidium iodide (KeyGen BioTech, KGA511) at 4°C, 30 min in the dark via flow cytometry (FCM) analysis.

Cell migration and invasion assays. Cell migration was assessed by a wound healing assay (22). Briefly, the indicated cells were seeded, cultured overnight until over 95% confluency, and then wounded with a pipette tip. The media were changed to remove cell debris, and images were captured at 24 and 48 h post-wounding. Cell invasion was assessed using the Matrigel Invasion Chamber (BD Biosciences) according to the manufacturer's instructions. The cells (1x10⁵) were re-suspended in serum-free media and placed on each Transwell membrane filter insert, with the lower chamber filled with complete medium. After 24-h incubation, the cells were stained with 0.005% crystal violet at room temperature for 10 min and counted under a microscope.

Statistical analysis. Data were presented as the mean ± standard deviation of at least three independent experiments, using SPSS 19.0 version (SPSS, Inc.). Groups with different treatments were compared using a two-tailed Student's t-test. ANOVA was used to compare more than two groups, and Bonferroni test was used in the post-hoc comparison. The expression of TELO2 between cancer tissue and adjacent normal tissue was compared using a two-independent non-parametric test (Mann-Whitney U test) in the IHC assay, a heatmap was used to present the expression correlations between two proteins. Kaplan-Meier and log rank tests were used to analyze the survival difference. Correlation analyses for the quantification of TELO2 and RICTOR staining were performed using Spearman's correlation. The corresponding relationship between TELO2 expression and CRC clinical features was analyzed by a Chi-square test. P<0.05 indicated a statistically significant difference.

Results

TELO2 was expressed at higher levels in CRC. In the GPL570 platform (HG-U133_Plus_2) of the GENT2 database (23), we found that the mRNA level of TELO2 was upregulated in adrenal gland, bladder, bone, breast, colon, liver, lung, muscle, pancreas, and skin cancer tissues in relation to corresponding normal tissues. The fold-change expression of TELO2 in colon normal tissues was 0.509 lower than cancerous tissues (P<0.001). No similar results were observed in esophageal and gastric cancers (Fig. 1A), indicating that TELO2 may be specifically associated with colon cancer in the GI tract. We collected four pairs of human CRC tissues and matched non-cancerous mucosa and assessed the expression of TELO2 by western blotting. As shown in Fig. 1B, all of the cancer tissues presented a higher expression level of TELO2 as compared with their corresponding non-cancerous controls. An IHC assay also showed higher expression levels of TELO2 in a CRC tissue array, and TELO2 was located in both the cytoplasm and nucleus (Fig. 1C). Fig. 1D shows the statistical difference in the expression scores between colorectal cancer and normal tissues.

TELO2 correlated with age, lymph node metastasis, and TNM stage in CRC patients. The correlation between TELO2 expression levels of CRC samples and a set of clinicopathological characteristics, including age, sex, tumor size, tumor location, histologic type, histology, T stage, N stage, and TNM stage, were analyzed using a Chi-square test (Table I). TELO2 was expressed at higher levels in CRC tissues. In our cohort of patients, there was positive TELO2 expression in 89 cases, and negative TELO2 expression in 11 cases. The expression of TELO2 was higher in older patients, negative lymph node metastasis, or local stages (I and II) of TNM (92.11, 96.15 and 96.08%, respectively) as compared to younger patients, positive lymph node metastasis, or advanced stages (III and IV) of TNM (79.17, 81.25 and 81.63%, respectively) (P<0.05). TELO2-positive patients trended towards a longer overall survival (OS) time than the TELO2-negative cohort, although this distinction was not significantly different between the two groups (Fig. 1E).

TELO2 induced malignant biological behavior in CRC. We searched the TELO2 gene level in cancer cell lines using the GENT2 database. LoVo cells expressed TELO2 at the highest level out of six different CRC cell lines including CACO2, COLO205, HCT116, HT29, LoVo, and SW480 (Table SI). To assess the effect of TELO2 on the malignant behavior of CRC cells *in vitro*, we established a stable LoVo cell line transfected with TELO2 shRNA or scrambled shRNA. A WST-1 and soft agar assay were performed to detect the proliferation and anchorage-independent growth ability, respectively. Our results showed that TELO2 downregulation significantly inhibited the proliferation and colony-forming capacity of LoVo CRC cells (Fig. 2A and B). In order to assess the effect of TELO2 downregulation on the cell cycle of CRC cells, flow cytometry was performed. Compared with the cells transfected with scrambled shRNA, LoVo cells transfected with TELO2-shRNA exhibited cells in the G1/S stage, while no statistical difference was detected (Fig. 2C). To examine
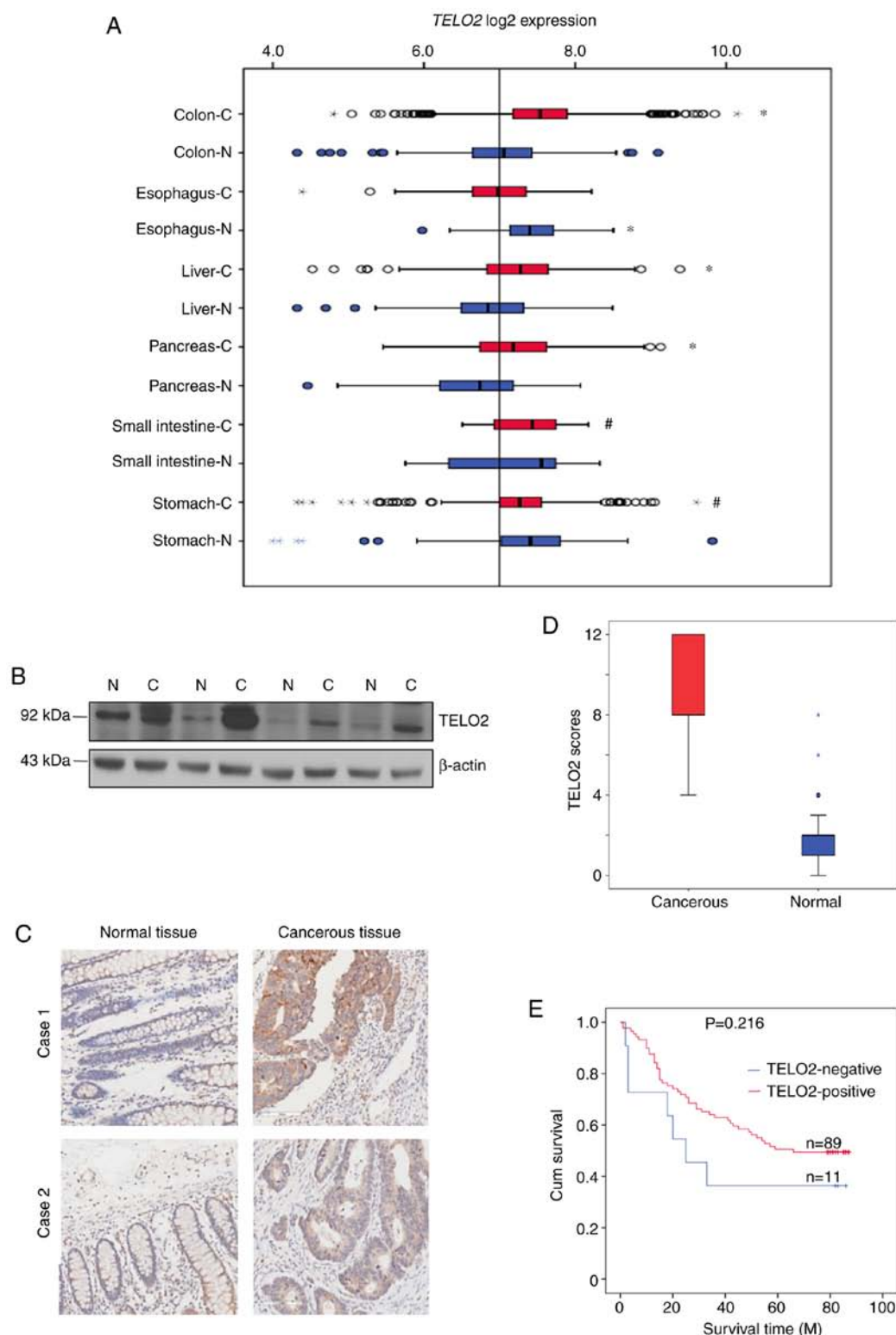
Figure 1. TELO2 was expressed at high levels in colorectal cancer (CRC) cells. (A) The expression pattern of TELO2 mRNA in normal (N) and cancerous (C) tissues of the digestive system. The boxes represent median expression, and the dots represent outliers. *Significant increase in TELO2 expression as compared with the indicated paired tissue. #No significant difference between the pair. (B) Four pairs of resected tumors and adjacent non-tumor tissue specimens were subjected to protein extraction and western blot analysis. N represents normal tissues, and C represents cancer tissues. (C) In two selected CRC patients, there was a higher expression of TELO2 in cancer tissues as confirmed by IHC. The magnification of the image is x200, and the scale bars are 100 μm. (D) The expression difference between cancer tissues (n=100) and non-cancerous tissues (n=80) (*P<0.001). (E) Log-rank analysis was used to detect the survival difference between TELO2-positive and -negative patients (P=0.216).

cell migration and invasion *in vitro*, we used a wound healing assay and Transwell matrix-coated cell culture inserts. After the downregulation of TELO2, the mobility and invasiveness of LoVo cells decreased as compared with the control cells (Fig. 2D and E). These data indicated that TELO2 downregulation inhibited the malignant biological behavior of CRC cells.

Table I. Difference of clinical characteristics in TELO2-positive and -negative patients.

Parameters	Total (N)	TELO2 (+)	TELO2 (-)	P-value
Age (y)	100	68.31±10.810	59.55±7.118	0.010[a]
Sex	100			0.757
Male	58	51	7	
Female	42	38	4	
Tumor sizes (cm)	100	5.62±2.177	5.35±2.14	0.707
Tumor location	100			0.750
Left	42	36	6	
Right	58	53	5	
Histologic grade	100			0.073
Grade 1	17	15	2	
Grade 2	74	68	6	
Grade 3	9	6	3	
Histology	100			0.392
Tubular	83	75	8	
Mucinous	17	14	3	
T stage	100			0.753
T1 + T2	0+4	0+4	0	
T3 + T4	64+32	57+28	11	
N stage	100			0.043[a]
N0	52	50	2	
N1 + N2	36+12	30+9	9	
TNM stage	100			0.045[a]
I + II (local stage)	4+47	4+45	2	
III + IV (advanced stage)	44+5	37+3	7	

[a]Statistically significant difference.

RICTOR bound to TELO2 and was positively correlated with TELO2 in CRC. Using a STRING database, we found that >10 proteins probably bound with TELO2. The combined score between RICTOR and TELO2 was 0.925 (Fig. 3A). Based on this analysis, a Co-IP assay was performed to detect the binding between the two proteins. We demonstrated that TELO2 bound with RICTOR in cells treated with CHAPS lysis buffer, which maintained the integrity of the mTORC2 complex (Fig. 3B). The location of TELO2 was further confirmed via an IHC assay and a tissue array. As shown in Fig. 3C, the expression of TELO2 was located in both the nucleus and cytoplasm, while RICTOR expression was mainly identified in the cytoplasm. Moreover, the expression location of RICTOR and TELO2 in CRC tissue cells was similar, which is indicated by the arrows. After scoring, we analyzed the data by Spearman's correlation (Fig. 3D and E), which showed that RICTOR was positively associated with TELO2 in both CRC tissue and adjacent normal colonic mucosa. A heatmap further confirmed the positive relationship between these two proteins (Fig. 3F).

Inhibition of RICTOR reversed TELO2-induced tumorigenesis in vitro. To verify whether RICTOR was required for TELO2-induced malignant behavior in CRC, we employed a RICTOR knockdown strategy in TELO2-overexpressed LoVo cells *in vitro*. As shown in Fig. 4A and B, TELO2 overexpression increased the proliferation and anchorage-independent growth ability, while transient transfection with RICTOR siRNA decreased the proliferation and anchorage-independent growth ability. Knock-down of RICTOR also blocked LoVo-Myc-TELO2 stable cells in the G1 phase of the cell cycle, which led to cell cycle arrest or death (Fig. 4C). Similar results were observed where the induction of metastatic phenotypes caused by the overexpression of TELO2 was abolished by the inhibition of RICTOR, as evidenced by the wound healing and Transwell chamber assays (Fig. 4D and E).

TELO2 induced tumorigenesis through mTORC2 activity with serum supplement. LoVo cells were stably transfected with TELO2 shRNA and cultured in conventional medium. Whole cell lysates were harvested, and western blot analysis was performed. Inhibition of TELO2 only decreased mTOR expression without changing RICTOR and RAPTOR levels (Fig. 5A). Additionally, levels of phosphorylated Akt Ser473, a protein downstream of mTORC2, was decreased, while the target proteins of mTORC1, p-S6K1 and p-4EBP1, were changed slightly under the treatment. However, no significant change was demonstrated in those cells without serum supplement, except for p-4EBP1 with a distinctive decrease (Fig. 5B). We then knocked down RICTOR using siRNA, and our results indicated that RICTOR downregulation inhibited TELO2
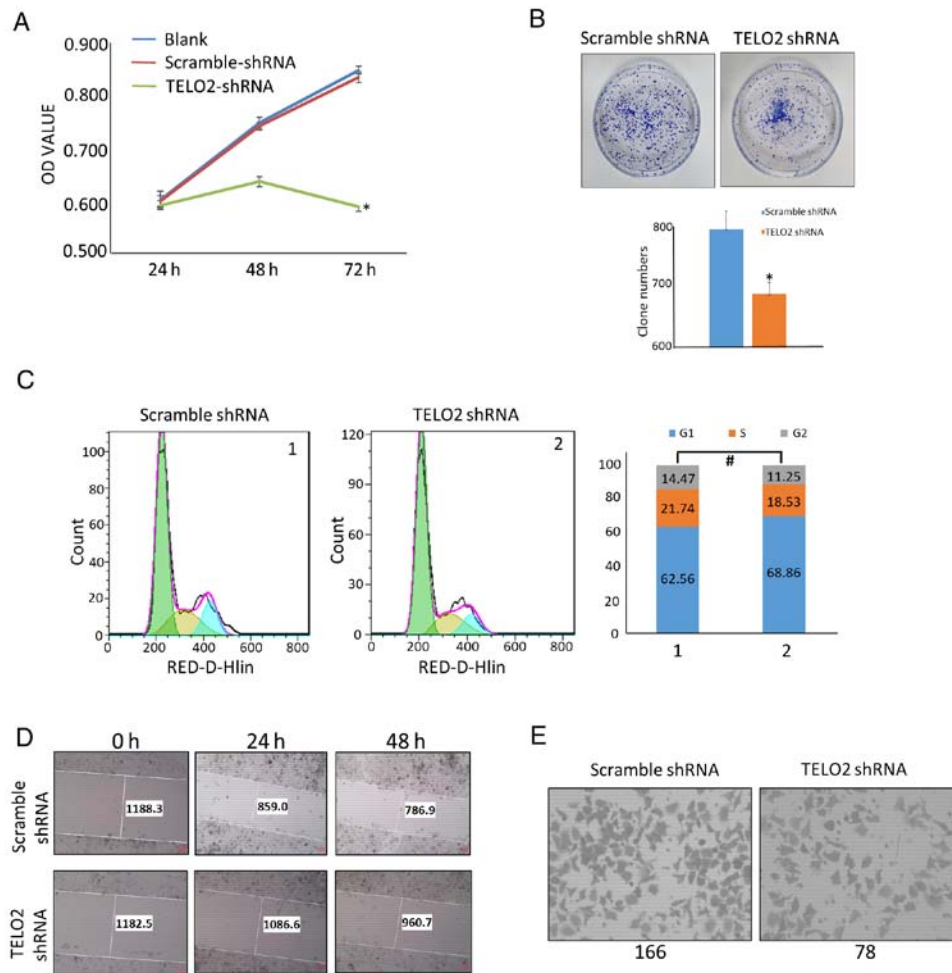
Figure 2. TELO2 acted as an oncogene in CRC. (A) LoVo cells were transfected with scrambled shRNA or TELO2 shRNA, and a WST-1 assay was used to detect the proliferation difference between the three groups (*P<0.05). (B) TELO2-silenced LoVo cells (1.5x10³) were plated in tissue culture dishes with soft agar. After 14 days, cell colonies were visualized by staining with crystal violet. Colony counts are in the right panel (*P<0.05). (C) The cell cycle distribution of transfected LoVo cells was analyzed by FCM, and the percentage cells in the different stages were marked (#P>0.05). (D) Images of the wound closure of LoVo cell monolayers transfected with indicated shRNA. (E) The invasive potential of LoVo cells transfected with scrambled shRNA or TELO2 shRNA was assessed, and the images were captured at x200 magnification. The experiments were repeated at least three times.

slightly and pAktS473 when cultured under normal conditions, while the expression of TELO2 was increased in RICTOR knockdown cells under serum deprivation (Fig. 5C). RT-PCR demonstrated that expression of RICTOR had no effect on the mRNA level of TELO2 in both normal or serum-deprived cultures (Fig. 5D).

RICTOR degraded TELO2 by ubiquitination under serum deprivation. To address the mechanism of how RICTOR affected the protein level of TELO2, we investigated the stability of TELO2 protein using a CHX chase assay. Time-course experiments showed that the stability of TELO2 was higher in cells with serum in the culture as compared with cells under serum deprivation. The half-life of TELO2 was further prolonged in LoVo cells transfected with RICTOR siRNA as compared with cells transfected with scrambled siRNA when cultured without serum. This function was reduced in cells cultured with a serum supplement (Fig. 6A and B). We then performed *in vitro* ubiquitination assays to further address whether RICTOR promoted the ubiquitination of TELO2. His-ubiquitin and/or RICTOR siRNA were transfected transiently, and knockdown of RICTOR reduced the ubiquitination

of both TELO2 with no serum culture (Fig. 6C). More importantly, the binding of RICTOR and TELO2 was increased in serum-deprived cells as compared with cells that were grown with serum in the culture, and mTOR was not present in this compound (Fig. 6D).

TELO2 functioned as double-edged sword in CRC. In Fig. 6E, we concluded the two-sides functions of TELO2 under different conditions in CRC. In normal condition with growth factors during in the progression of CRC, TELO2 binds with RICTOR as mTORC2 complex in promoting proliferation, migration and invasion by AKT pathway. However, in serum deprivation usually happened under a heavy burden of tumor, TELO2 is ubiquitinated by RICTOR through an mTORC2-independent manner.

Discussion

In the present study, we characterized the role and partial mechanism of TELO2 in CRC progression. TELO2 was expressed at high levels in CRC. Inhibition of TELO2 resulted in the reduction of tumorigenesis in CRC cells, but no difference was shown in the OS between TELO2-positive and
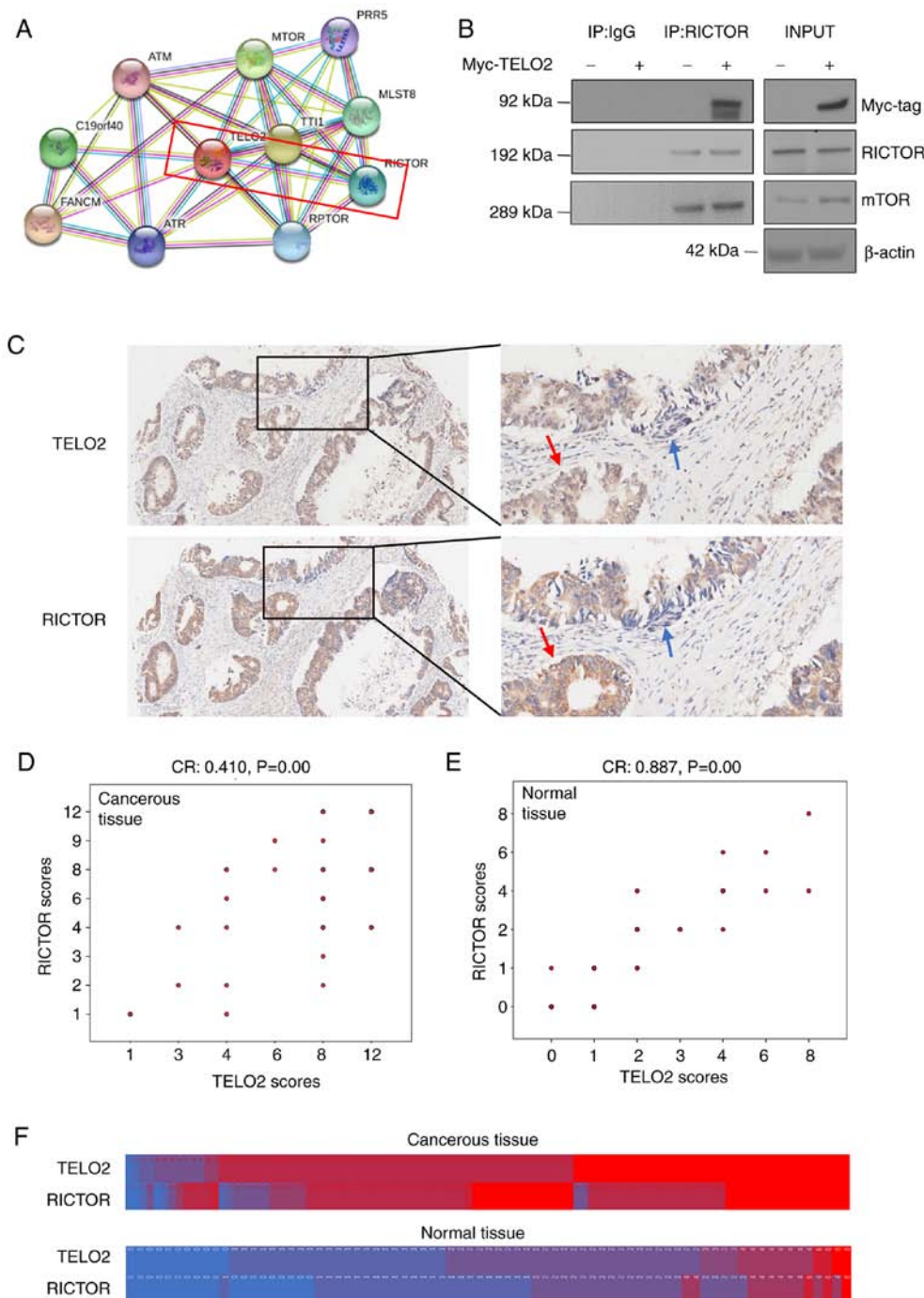
Figure 3. RICTOR bound to TELO2, and its expression was positively correlated with TELO2 in CRC. (A) Potential TELO2-binding partners were predicted using a STRING database. Red boxes represent protein-protein interactions. (B) LoVo cells were transfected with Myc-TELO2 or pLPC-Myc. CHAPS lysis buffer was used to prepare whole cell lysates, and immunoprecipitation was performed to detect the interaction between TELO2 and RICTOR. The experiments were repeated twice. (C) An immunohistochemistry assay was performed to investigate TELO2 and RICTOR expression in serial sections of cancer tissue from one patient (x200). The red arrow shows high expression of both TELO2 and RICTOR, and the blue arrow shows low expression of both TELO2 and RICTOR. (D and E) Spearman correlation analysis was performed to test the expression relevance between TELO2 and RICTOR in CRC tissues (n=100) and adjacent normal tissues (n=77). (F) A heat map shows the correlation between TELO2 and RICTOR expression.

-negative patients. The TELO2 expression rate was positively correlated with age and negatively correlated with lymph node metastasis and TNM stage at the same time. To the best of our knowledge, these results indicated, for the first time, that TELO2 expression is higher during the local stages of CRC and leads to tumorigenesis and metastasis, while the expression rate of TELO2 is decreased during the advanced stages of CRC progression with lymph node and organ metastasis. The

differential expression of TELO2 during the various stages of CRC offset its role in the prognosis suggesting that TELO2 plays a distinctive role in the development of CRC. The role of TELO2 in the prognosis of CRC, which differs from that in breast cancer (14), is still unclear, indicating that mechanism of TELO2 is different in various cancers.

Next, we needed to confirm the mechanism of TELO2-induced cancer progression in CRC. TELO2 and Tti1 play a critical role
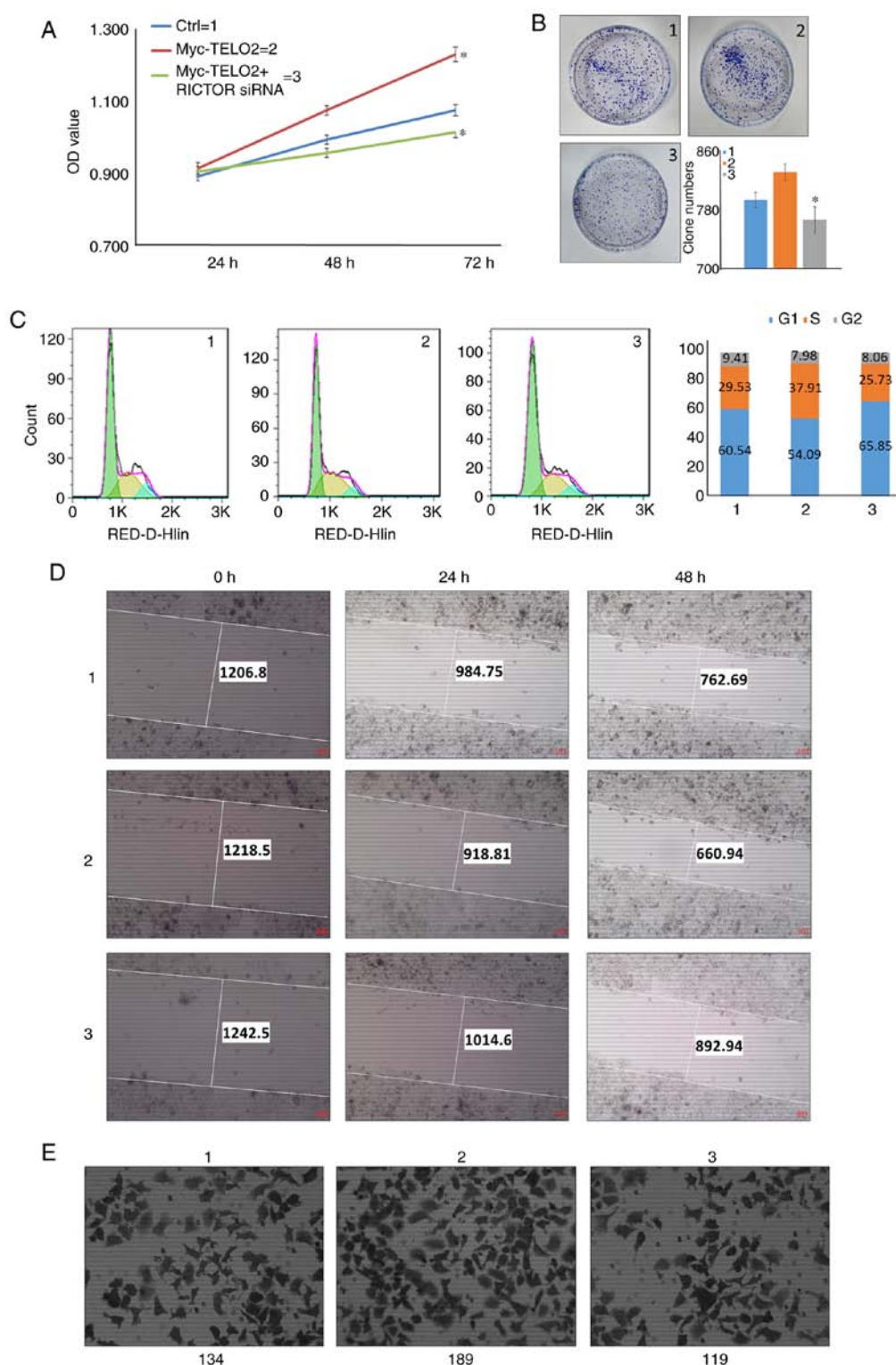
Figure 4. Knockdown of RICTOR inhibited TELO2-induced tumorigenesis in CRC. Stable Myc-TELO2 LoVo cells were transfected with RICTOR-siRNA. The experimental groups, including ctrl, Myc-TELO2, and Myc-TELO2 plus RICTOR-siRNA, were defined as groups 1, 2, and 3, respectively. (A) A WST-1 assay was used to detect the proliferation rate at different times ($^*P<0.05$). (B) A soft agar assay was preformed to detect tumorigenic ability. The number of colonies for the different transfections are shown below the panel ($^*P<0.05$). (C) Flow cytometry was performed to investigate the cell cycle distribution, and the right panel shows the percentage of cells in the different stages. (D) Wound healing assay was used to investigate the migration ability. The numbers mark the interval distance after scratching at the indicated time points. (E) A Transwell chamber assay was used to detect the invasion ability, and the numbers below indicate the invaded cells in each chamber. All of the experiments were performed three times.

in mTOR complex formation (10). mTORC1, mainly containing mTOR, RAPTOR (regulatory protein associated with mTOR), and mLST8 (mammalian lethal with Sec13 protein 8), regulates cell growth and metabolism through two key effectors, p70S6 Kinase 1 (S6K1) and eIF4E binding protein (4EBP) (24,25). mTORC2, including mTOR, RICTOR, and mLST8, controls proliferation, survival, and migration by phosphorylating the AGC subfamily of protein kinases (a subgroup of Ser/Thr protein
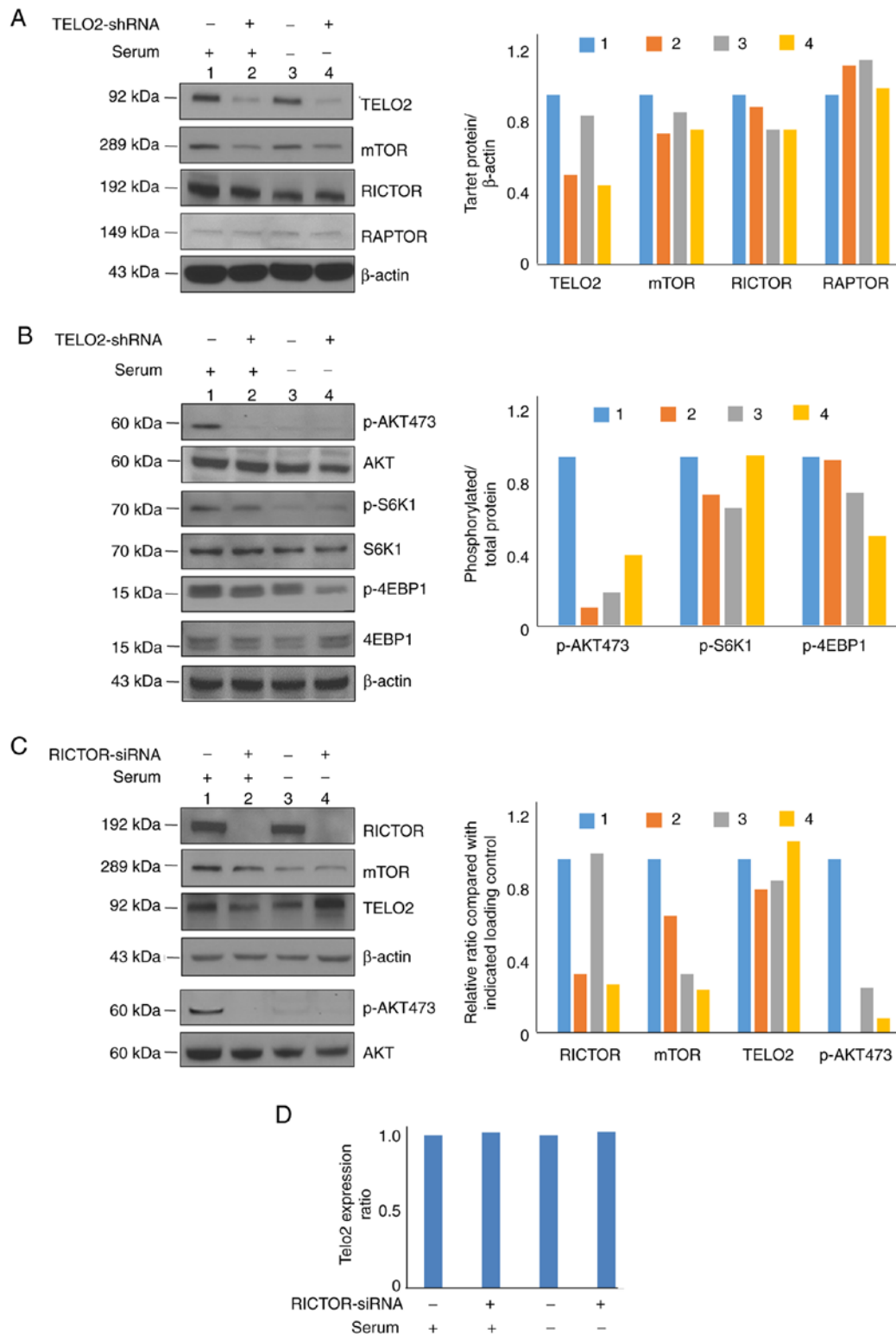
Figure 5. TELO2 induced tumorigenesis mainly through mTORC2 with serum. (A and B) LoVo cells stably transfected with scrambled shRNA or TELO2 shRNA were cultured with 10% FBS or 0.02% FBS for 24 h. Whole cell lysates were prepared, and western blot analysis was performed to detect the indicated proteins, right panel presented the relative gray value of each target blot. (C) LoVo cells were transfected with scrambled siRNA or RICTOR siRNA, cultured with or without serum for 24 h, and then mTORC2-related proteins were detected using western blot analysis, right panel presented the relative gray value of each target blot. The p-AKT was normalized to the AKT protein. (D) The expression of TELO2 in LoVo cells transfected with scrambled siRNA or RICTOR siRNA was determined by qPCR. All of the experiments were performed twice.

kinases based on sequence alignments of their catalytic kinase domain), including Akt at Ser473 (16,26). It has been previously reported that TELO2 stabilizes mTORC1-substrate interactions to activate T cell and mitogenic signaling (7). However, no studies

have shown the role of TELO2 in mTORC2. In the present study, a positive correlation between TELO2 and RICTOR protein was identified. Inhibition of RICTOR attenuated TELO2-induced proliferation, cell cycle progression, invasion, and migration in
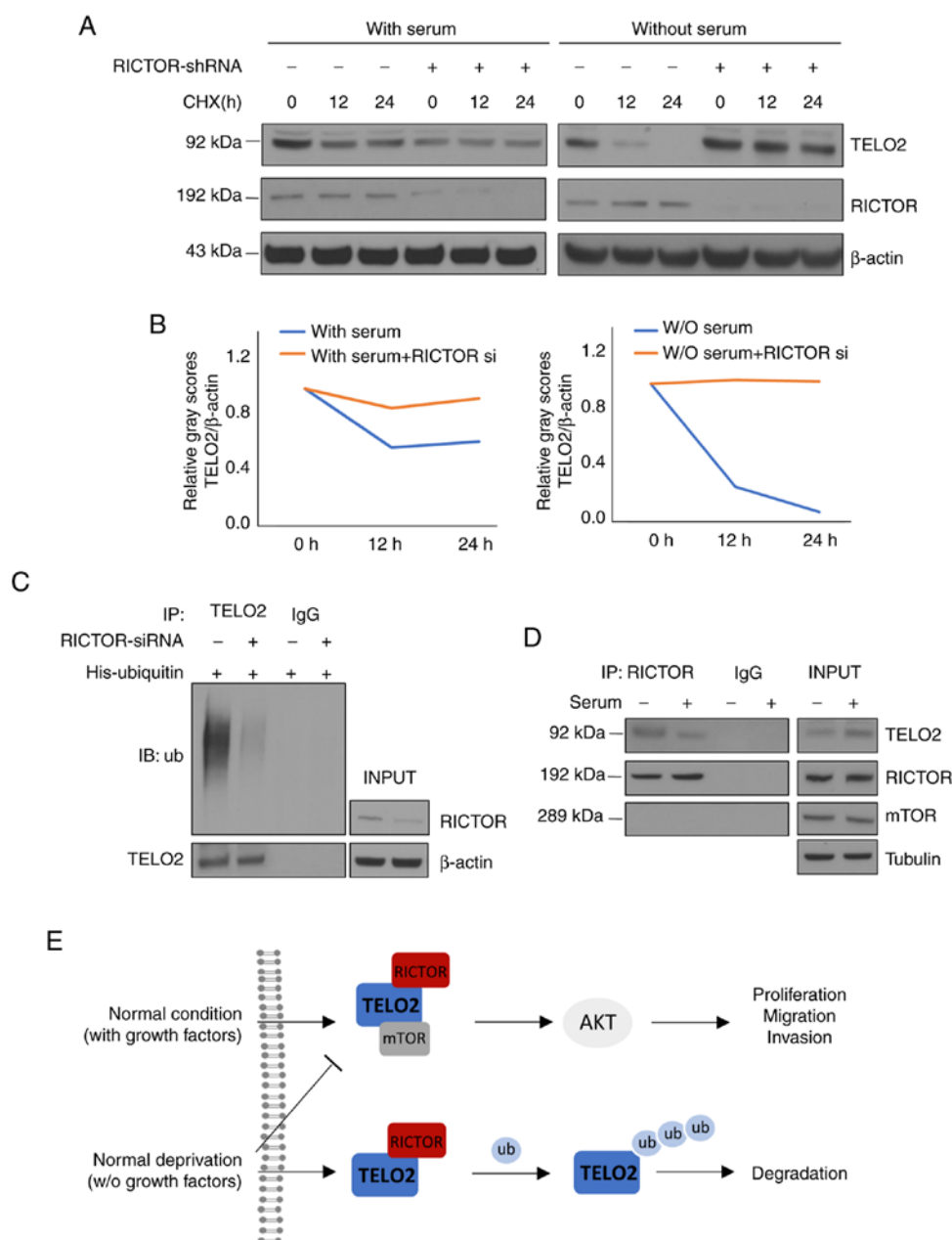
Figure 6. RICTOR degraded TELO2 by ubiquitination under serum deprivation. (A) LoVo cells were transfected with scrambled siRNA or RICTOR siRNA and cultured with or without serum for 24 h. CHX (50 μg/ml) was added to block protein synthesis at different time points, and the protein levels of TELO2 or RICTOR were examined by western blot analysis. (B) ImageJ software was used to scan the grey scores of TELO2 expression, and a line chart was drawn to present the change in the difference of TELO2 expression between the groups. (C) LoVo cells containing scrambled siRNA or RICTOR siRNA were transfected with His-ubiquitin. Forty-four hours post-transfection, cells were incubated in serum-deprived conditions for an additional 24 h, and then 1% triton lysis buffer was used to lysate the cells. Immunoprecipitation analysis was performed using a TELO2 antibody, and normal IgG was used as a negative control. (D) LoVo cells were incubated with or without serum for 24 h, and then 1% triton lysis buffer was used to lysate the cells. Immunoprecipitation analysis was performed using a RICTOR antibody, and normal IgG was used as a negative control. All of the experiments were performed twice. (E) The graphical abstract clarified the role of TELO2 by RICTOR in CRC progression under different conditions.

CRC cells. These data indicated that TELO2 induces tumorigenesis mainly via binding with RICTOR, a mTORC2-specific member, and dissociation of this compound could repress the oncogenic ability of TELO2.

Finally, we studied the binding pattern of TELO2 and RICTOR in CRC under different conditions. Nutrients and growth factors are usually supplied by the bloodstream in solid tumors, and growth factors are the only well-defined stimulus for mTORC2 through the phosphorylation of Akt (27). Akt plays a strong carcinogenic role by either inducing or inhibiting

downstream transcription factors (28,29). However, inhibition of mTOR by nutrient- or serum-deprivation stimulates the ubiquitin proteasome system to degrade ubiquitinated proteins (30). In addition, RICTOR was originally identified as a specific binding partner of mTOR that regulates the cytoskeleton and phosphorylates Akt. Multiple complexes containing RICTOR have been identified as mTORC2-independent with oncogenic actions (31,32). For example, RICTOR is proposed to be a scaffold protein for integrin-linked kinase (ILK) and appears to be mandatory for TGFb-1-mediated epithelial-mesenchymal

transition (33). Another RICTOR-containing complex is composed of tetraspanin 8 and integrin a3, which is required for the assembly and function of the mTORC2 complex in glioma cells (34). Interestingly, RICTOR forms a complex with Cullin-1 to enhance its E3 ligase activity and promote serum/glucocorticoid-induced kinase (SGK) ubiquitination (35). Our previous study indicated that RICTOR and FBXW-7, an E3 ligase complex, exert anti-oncogenic activities by promoting the degradation of c-Myc and cyclin E in CRC cells without serum supplementation (36). Thus, this study investigated that inhibition of TELO2 under normal culture conditions, which mainly reduced the activity of Akt, with a slight change in 4EBP1 and S6K1. This effect was reduced with serum deprivation, indicating that the TELO2/RICTOR complex induced cell survival, proliferation, and migration during CRC progression in a serum-dependent manner via the mTORC2 pathway. In addition, RICTOR functioned as an E3 adaptor and degraded TELO2 under serum-deprived culture conditions, further confirming that TELO2 was ubiquitinated in an mTOR-independent manner. However, identification of the TELO2 and RICTOR binding site would allow for further evaluation of the mechanism of the TELO2/RICTOR complex during serum deprivation.

In conclusion (Fig. 6E), our study demonstrated that TELO2 functions as a trigger of CRC progression through mTORC2, particularly RICTOR in normal cultural conditions. However, this effect could be reversed with serum deprivation, which is common in solid tumor progression and partially supports the theory that TELO2 does not play a role in CRC prognosis. Thus, the present study provides evidence that TELO2 acts as a vital role in CRC growth and progression, and as such, may serve as a therapeutic target for CRC. This TELO2-driven therapy should be further confirmed for the functions of TELO2 in normal cells and its double-edged sword under different conditions yet.

Availability of data and materials

The datasets used and/or analyzed during the current study are available from the corresponding author upon reasonable request.

Authors' contributions

ZG, XZ, and HZ performed the experiments. XW, FT, LH, JZ, and ZG designed the study. JH reviewed the IHC results. NZ, XL, and YZ collected the patients' information and performed the statistical analysis. ZG wrote the manuscript. All of the authors approved the final version.

Ethics approval and consent to participate

The proposal of this study was approved by the Institutional Review Committee of Gannan Medical University. All of the patients signed informed consent for the use of their tissues.

Patient consent for publication

Not applicable.

Competing interests

There are no competing interests to be declared.

References

1. Siegel RL, Miller KD and Jemal A: Cancer statistics, 2019. CA Cancer J Clin 69: 7-34, 2019.
2. Lin SH, Raju GS, Huff C, Ye Y, Gu J, Chen JS, Hildebrandt MAT, Liang H, Menter DG, Morris J, et al: The somatic mutation landscape of premalignant colorectal adenoma. Gut 67: 1299-1305, 2018.
3. Marschner N, Zacharias S, Lordick F, Hegewisch-Becker S, Martens U, Welt A, Hagen V, Gleiber W, Bohnet S, Kruggel L, et al: Association of disease progression with health-related quality of life among adults with breast, lung, pancreatic, and colorectal cancer. JAMA Netw Open 3: e200643, 2020.
4. Chiorean EG, Nandakumar G, Fadelu T, Temin S, Alarcon-Rozas AE, Bejarano S, Croitoru AE, Grover S, Lohar PV, Odhiambo A, et al: Treatment of patients with late-stage colorectal cancer: ASCO resource-stratified guideline. JCO Glob Oncol 6: 414-438, 2020.
5. Runge KW and Zakian VA: TEL2, an essential gene required for telomere length regulation and telomere position effect in Saccharomyces cerevisiae. Mol Cell Biol 16: 3094-3105, 1996.
6. Saxton RA and Sabatini DM: mTOR signaling in growth, metabolism, and disease. Cell 169: 361-371, 2017.
7. Brown MC and Gromeier M: MNK controls mTORC1: Substrate association through regulation of TELO2 binding with mTORC1. Cell Rep 18: 1444-1457, 2017.
8. Takai H, Wang RC, Takai KK, Yang H and de Lange T: Tel2 regulates the stability of PI3K-related protein kinases. Cell 131: 1248-1259, 2007.
9. Bahrami A, Khazaei M, Hasanzadeh M, ShahidSales S, Joudi Mashhad M, Farazestanian M, Sadeghnia HR, Rezayi M, Maftouh M, Hassanian SM and Avan A: Therapeutic potential of targeting PI3K/AKT pathway in treatment of colorectal cancer: Rational and progress. J Cell Biochem 119: 2460-2469, 2018.
10. Kaizuka T, Hara T, Oshiro N, Kikkawa U, Yonezawa K, Takehana K, Iemura S, Natsume T and Mizushima N: Tti1 and Tel2 are critical factors in mammalian target of rapamycin complex assembly. J Biol Chem 285: 20109-20116, 2010.
11. Takai H, Xie Y, de Lange T and Pavletich NP: Tel2 structure and function in the Hsp90-dependent maturation of mTOR and ATR complexes. Genes Dev 24: 2019-2030, 2010.
12. Fernandez-Saiz V, Targosz BS, Lemeer S, Eichner R, Langer C, Bullinger L, Reiter C, Slotta-Huspenina J, Schroeder S, Knorn AM, et al: SCFFbxo9 and CK2 direct the cellular response to growth factor withdrawal via Tel2/Tti1 degradation and promote survival in multiple myeloma. Nat Cell Biol 15: 72-81, 2013.
13. Morais-Rodrigues F, Silv Erio-Machado R, Kato RB, Rodrigues DLN, Valdez-Baez J, Fonseca V, San EJ, Gomes LGR, Dos Santos RG, Vinicius Canário Viana M, et al: Analysis of the microarray gene expression for breast cancer progression after the application modified logistic regression. Gene 726: 144168, 2020.
14. Feng SW, Chen Y, Tsai WC, Chiou HC, Wu ST, Huang LC, Lin C, Hsieh CC, Yang YJ and Hueng DY: Overexpression of TELO2 decreases survival in human high-grade gliomas. Oncotarget 7: 46056-46066, 2016.
15. Gala MK, Mizukami Y, Le LP, Moriichi K, Austin T, Yamamoto M, Lauwers GY, Bardeesy N and Chung DC: Germline mutations in oncogene-induced senescence pathways are associated with multiple sessile serrated adenomas. Gastroenterology 146: 520-529, 2014.

16. Sarbassov DD, Guertin DA, Ali SM and Sabatini DM: Phosphorylation and regulation of Akt/PKB by the rictor-mTOR complex. Science 307: 1098-1101, 2005.
17. Yang G, Murashige DS, Humphrey SJ and James DE: A positive feedback loop between Akt and mTORC2 via SIN1 phosphorylation. Cell Rep 12: 937-943, 2015.
18. Lampada A, O'Prey J, Szabadkai G, Ryan KM, Hochhauser D and Salomoni P: mTORC1-independent autophagy regulates receptor tyrosine kinase phosphorylation in colorectal cancer cells via an mTORC2-mediated mechanism. Cell Death Differ 24: 1045-1062, 2017.
19. Wang L, Qi J, Yu J, Chen H, Zou Z, Lin X and Guo L: Overexpression of rictor protein in colorectal cancer is correlated with tumor progression and prognosis. Oncol Lett 14: 6198-6202, 2017.
20. Creytens D: NKX2.2 immunohistochemistry in the distinction of ewing sarcoma from cytomorphologic mimics: Diagnostic utility and pitfalls-comment on russell-goldman et al. Cancer Cytopathol 127: 202, 2019.
21. Zhao Y, Zhang W, Guo Z, Ma F, Wu Y, Bai Y, Gong W, Chen Y, Cheng T, Zhi F, *et al*: Inhibition of the transcription factor Sp1 suppresses colon cancer stem cell growth and induces apoptosis *in vitro* and in nude mouse xenografts. Oncol Rep 30: 1782-1792, 2013.
22. Chen Y, Liu J, Wang W, Xiang L, Wang J, Liu S, Zhou H and Guo Z: High expression of hnRNPA1 promotes cell invasion by inducing EMT in gastric cancer. Oncol Rep 39: 1693-1701, 2018.
23. Park SJ, Yoon BH, Kim SK and Kim SY: GENT2: An updated gene expression database for normal and tumor tissues. BMC Med Genomics 12 (Suppl 5): S101, 2019.
24. Carroll B: Spatial regulation of mTORC1 signalling: Beyond the Rag GTPases. Semin Cell Dev Biol 107: 103-111, 2020.
25. Rabanal-Ruiz Y and Korolchuk VI: mTORC1 and nutrient homeostasis: The central role of the lysosome. Int J Mol Sci 19: 818, 2018.
26. Li X and Gao T: mTORC2 phosphorylates protein kinase Cζ to regulate its stability and activity. EMBO Rep 15: 191-198, 2014.
27. Knudsen JR, Fritzen AM, James DE, Jensen TE, Kleinert M and Richter EA: Growth factor-dependent and -independent activation of mTORC2. Trends Endocrinol Metab 31: 13-24, 2020.
28. Manning BD and Toker A: AKT/PKB signaling: Navigating the network. Cell 169: 381-405, 2017.
29. Jia R and Bonifacino JS: Lysosome positioning influences mTORC2 and AKT signaling. Mol Cell 75: 26-38.e3, 2019.
30. Zhao J, Zhai B, Gygi SP and Goldberg AL: mTOR inhibition activates overall protein degradation by the ubiquitin proteasome system as well as by autophagy. Proc Natl Acad Sci USA 112: 15790-15797, 2015.
31. Gkountakos A, Pilotto S, Mafficini A, Vicentini C, Simbolo M, Milella M, Tortora G, Scarpa A, Bria E and Corbo V: Unmasking the impact of Rictor in cancer: Novel insights of mTORC2 complex. Carcinogenesis 39: 971-980, 2018.
32. Zhang S, Qian G, Zhang QQ, Yao Y, Wang D, Chen ZG, Wang LJ, Chen M and Sun SY: mTORC2 suppresses GSK3-dependent snail degradation to positively regulate cancer cell invasion and metastasis. Cancer Res 79: 3725-3736, 2019.
33. Serrano I, McDonald PC, Lock FE and Dedhar S: Role of the integrin-linked kinase (ILK)/Rictor complex in TGFβ-1-induced epithelial-mesenchymal transition (EMT). Oncogene 32: 50-60, 2013.
34. Pan SJ, Zhan SK, Pan YX, Liu W, Bian LG, Sun B and Sun QF: Tetraspanin 8-rictor-integrin α3 complex is required for glioma cell migration. Int J Mol Sci 16: 5363-5374, 2015.
35. Gao D, Wan L, Inuzuka H, Berg AH, Tseng A, Zhai B, Shaik S, Bennett E, Tron AE, Gasser JA, *et al*: Rictor forms a complex with Cullin-1 to promote SGK1 ubiquitination and destruction. Mol Cell 39: 797-808, 2010.
36. Guo Z, Zhou Y, Evers BM and Wang Q: Rictor regulates FBXW7-dependent c-Myc and cyclin E degradation in colorectal cancer cells. Biochem Biophys Res Commun 418: 426-432, 2012.